Assessment of Extending a Two-Port Calibration to a Multi-Port Microwave Scanner

Assessment of Extending a Two-Port Calibration to a Multi-Port Microwave Scanner

M. Gugliermino*, D. O. Rodriguez-Duarte*, C. Origlia*, J. A. Tobon Vasquez*,
R. Scapaticci†, L. Crocco†, F. Vipiana*
*Dept. Electronics and Telecommunications, Politecnico di Torino, Torino, Italy
†Institute for Electromagnetic Sensing of the Environment, National Research Council, CNR, Naples, Italy
francesca.vipiana@polito.it

***Abstract*—This work evaluates a sub-calibration method for a multi-port microwave imaging scanner. This decreases the complexity of a conventional full n-port calibration, albeit inserting uncertainties. The approach involves a combined 2-port full standard calibration along with a multi-port extension. It addresses systematic errors and reduces the impact of losses and phase shifts introduced by the multiplexing component of a microwave scanner, normally interfacing the 2-port transceiving stage with the multiple radiating elements. The analysis examines the calibration assumptions and validates them on a microwave scanner utilizing a 2-port vector network analyzer and a 2×22 solid-state switching matrix. Repeatability and stability tests confirm the calibration's reliability, effectiveness, and permissible effect on the imaging retrieval capabilities.**

***Index Terms*—Biomedical microwave imaging, calibration technique, propagation, solid-state switches.**

I. Introduction

Microwave imaging (MWI) is a technology that exploits dielectric contrasts to generate images of the interior of inaccessible domains. This has shown potential in biomedical applications such as breast cancer screening and diagnosing and monitoring brain strokes [1], where contrasts between healthy and pathological tissues are presented.

A generic MWI scanner comprises four main components: 1) a control unit (e.g., a laptop) that oversees data collection and executes imaging algorithms; 2) a transceiver system responsible for generating signals and capturing their back-scattered responses, known as scattering parameters; 3) radiating elements, typically an array of antennas encircling the domain of interest (DoI); and 4) a multiplexing stage, commonly a switching matrix (Sw-M), that connects the transceiver to the radiating elements [2], as depicted in Fig. 1. This arrangement enables multi-view schemes, which are crucial for imaging algorithms. However, using a Sw-M requires carefully calibrating phase shifts and path losses.

In general, the imaging algorithms model the reference phase at the antenna ports, but in practical implementation, this is affected by cables, switching matrix, and other components [3], [4]. For this reason, calibration is a crucial step, which aligns the measurement reference plane with the input plane of the antennas, P_1 and P_2, A_1 and A_n, respectively, in the scheme in Fig. 1.

In many MWI applications, the device exploits an array of antennas in order to increase the amount of available data. In turn, this entails that conventional port-to-port calibration can become cumbersome and affect the overall efficiency of the system.

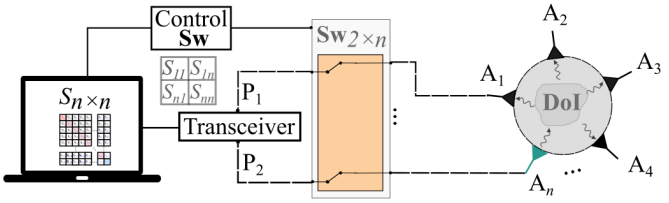

Fig. 1. MWI system scheme. From the left: a unit control, a transceiver, a switching matrix (**Sw**), and a generic DoI that is surrounded by n-antennas.

In this work, we introduce a sub-calibration designed for multi-port MWI systems. This method bypasses the need for the conventional full-port $n \times n$ calibration, which typically requires at least $4n-1$ measurements, where n is the number of radiating elements. We validated this method experimentally using a microwave imaging system for brain stroke monitoring, with a Vector Network Analyzer (VNA) as the transceiver, a Sw-M, and a setup of twenty-two radiating antennas.

II. Calibration Process

To perform the calibration, the first step (I) ensures the signal paths within the Sw-M are equivalent, which, in our case, is a solid state studied in [5]. The Sw-M provides 2×64 multiplexing channels, so we choose 2×22 of them with the same electrical path for each. Figure 2 shows the transmission coefficients of the selected channels going from one of the Sw-M inputs to the 22 respective outputs. The amplitude variation is approximately 0.1 dB, while the phase variation is around 0.05 degrees. It is worth noticing that in addition to the previous condition, we use the same kind of coaxial cables for all connections, guaranteeing the same lengths.

Next, the calibration follows a systematic two-step process: (II) a standard full 2-port calibration, such as a short-open-load-thru (SOLT) calibration [4], and (III) a calibration extrapolation. In II, a pair of channels is selected and then applied to a standard calibration, determining the corresponding calibration coefficients. This involves measuring known reference standards at the antenna ports, for example, using an electronic calibration module (E-Cal) [6], as done here. In

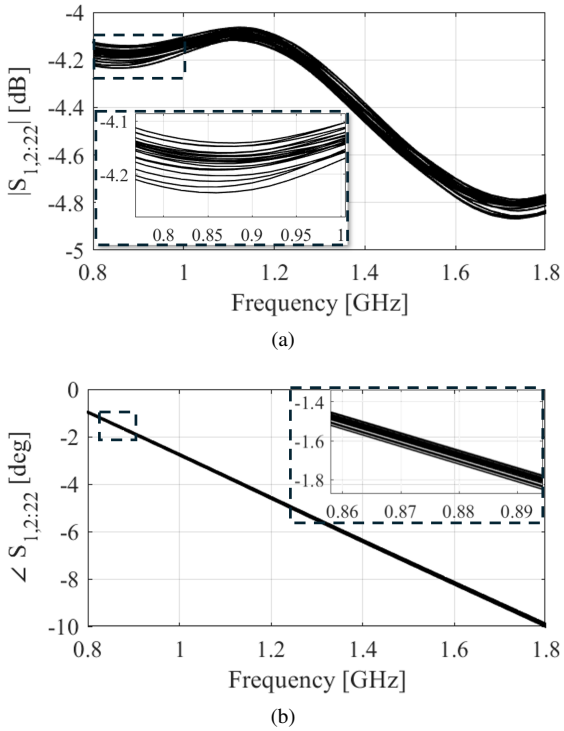

Fig. 2. Transmission coefficients of the 22 Sw-M selected paths: (a) amplitude in dB, and (b) phase in degrees.

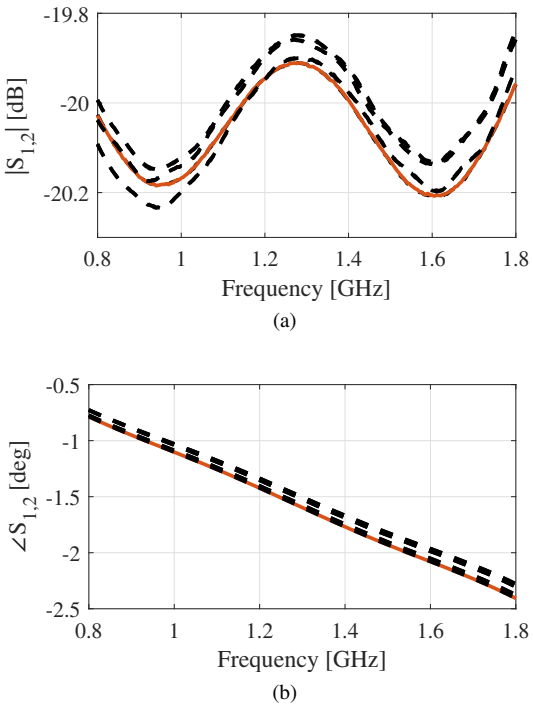

Fig. 3. Comparison of transmission coefficients applying the calibration: (a) magnitude in dB, and (b) phase in degrees. The red lines are the references, full-calibrated ones, and the black dotted lines are the ones where the proposed calibration is applied.

III, the calibration coefficients obtained are applied to all other antenna pairs, obtaining in a sub-calibrated 22×22 scattering matrix.

To verify that the error introduced by applying the calibration coefficient of one path to the others is negligible, we compare the transmission response in a controlled and analogous brain stroke monitoring measuring scenario. To this end, we set a 20 dB attenuator between Sw-M channels, mimicking the head effect, observing a maximum variation of about 0.2 dB in magnitude and 0.1 degrees in phase, as shown in Fig. 3. The red lines represent the measurements taken on the directly calibrated paths, while the dashed black lines correspond to sub-calibrated ones. Then, last, we check the imaging retrieval after applying the calibration.

III. Experimental Testing

For testing in an actual imaging scenario, we apply the calibration to a mimicked hemorrhage condition as in [7], using a MWI system consisting of a laptop, a 2-port compact VNA [8], a solid-state Sw-M [9], and an anthropomorphic head phantom surrounded by 22 antennas, and the inversion algorithm described in [7]. The experiment involves two stages, one representing the progression of a hemorrhagic stroke from a healthy state to a 20 cm^3 stroke and another from a 20 cm^3 to a 40 cm^3 stroke. Figure 4 presents the 3-D normalized contrast maps in two different scenarios, where the goal is to monitor a stroke positioned on the front-right side (frontal lobe), approximately 5 cm from the top of the head. The algorithm successfully identifies the correct location and progression of the stroke, as indicated by the white contours.

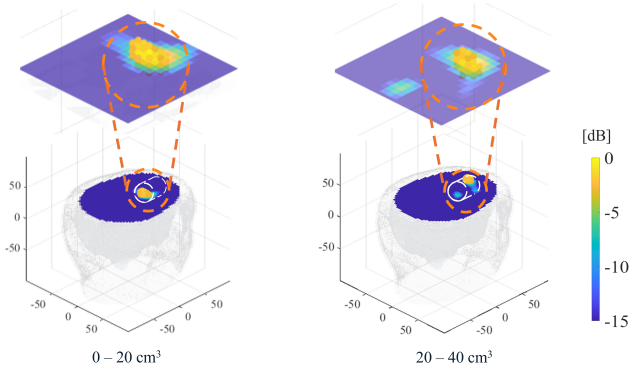

Fig. 4. Monitoring of hemorrhagic progression: 3-D normalized dielectric contrast applying the proposed calibration. The slices are cut in the middle of the stroke region of the case (a) healthy – 20 cm^3 and (b) 20 – 40 cm^3.

IV. Conclusions

This study has introduced and validated a simplified two-port calibration method for microwave imaging systems, significantly reducing the complexity and number of measurements required compared to traditional full-port calibration methods. This approach effectively compensates for systematic errors, phase shifts, and losses introduced by switching

matrices by leveraging a two-step process involving standard calibration and multi-port extrapolation. The method has been tested using a brain stroke monitoring system, demonstrating reliable performance and accuracy in data retrieval. The results confirmed the potential of the proposed calibration technique.

ACKNOWLEDGMENT

This work was supported in part by the project PON Research and Innovation "Microwave Imaging and Detection powered by Artificial Intelligence for Medical and Industrial Applications (DM 1062/21)", funded by MUR. It was carried out partially in part within the Agritech National Research Center, funded by the European Union Next-Generation EU (Piano Nazionale di Ripresa e Resilienza (PNRR) – MISSIONE 4 COMPONENTE 2, INVESTIMENTO 1.4 – D.D. 1032 17/06/2022, CN00000022); in part within the research project "MedWaveImage - Microwave imaging technology transfer to innovate the medical sector", funded by Interreg Central Europe (CE0200670) and in part within the research project "3BAtwin - Bone, Brain, Breast and Axillary Medical Microwave Imaging Twinning" funded by Horizon Europe Framework Programme (101159623). We thank Prof. J.Ch. Bolomey (University Paris-Saclay) for fruitful discussions and eV-Technologies for providing us with the correlators.

REFERENCES

[1] C. Origlia, D. O. Rodriguez-Duarte, J. A. Tobon Vasquez, J.-C. Bolomey, and F. Vipiana, "Review of microwave near-field sensing and imaging devices in medical applications," *Sensors*, vol. 24, no. 14, p. 4515, 2024.

[2] L. Guo, A. S. M. Alqadami, and A. Abbosh, "Stroke diagnosis using microwave techniques: Review of systems and algorithms," *IEEE Journal of Electromagnetics, RF and Microwaves in Medicine and Biology*, vol. 7, no. 2, pp. 122–135, 2023.

[3] S. Cathers, J. LoVetri, I. Jeffrey, and C. Gilmore, "Electromagnetic imaging system calibration with 2-port error models," *IEEE Open Journal of Antennas and Propagation*, vol. 4, pp. 1142–1153, 2023.

[4] V. Teppati, A. Ferrero, and M. Sayed, "Multiport s-parameters measurement methods," in *Modern RF and Microwave Measurement Techniques*, A. Ferrero and M. Sayed, Eds. Cambridge University Press, 2013, pp. 219–240.

[5] M. Gugliermino, D. Rodriguez-Duarte, C. Origlia, J. T. Vasquez, R. Scapaticci, J. C. Bolomey, L. Crocco, and F. Vipiana, "On the use of an electromechanical and a solid-state switching matrix for a portable microwave-based brain stroke scanner," *IEEE Antennas and Wireless Propagation Letters*, 2024.

[6] "Keysight datasheet," Available at https://www.keysight.com/us/en/product/N7551A/electronic-calibration-module-ecal-dc-6-5-ghz-2-port.html.

[7] D. O. Rodriguez-Duarte and et al., "Experimental assessment of real-time brain stroke monitoring via a microwave imaging scanner," *IEEE Open Journal of Antennas and Propagation*, vol. 3, pp. 824–835, 2022.

[8] "Streamline series vector network analyzer," Available at https://www.keysight.com/us/en/products/network-analyzers/streamline-series-usb-vector-network-analyzers/p50xxb-streamline-series-vector-network-analyzers.html.

[9] "Dual evt1016 datasheet," Available at https://ev-technologies.com/portfolio-items/dual-evt1016/.